 Helmholtz-Zentrum Geesthacht Centre for Materials and Coastal Research	DOC:	MERIS alternative atmospheric correction		
	DATE:	20110527		
	Issue:	1	Revision:	

Alternative Atmospheric Correction Procedure for Case 2 Water Remote Sensing using MERIS

ATBD V 1.0

Author: Roland Doerffer

Distribution: Ludovic Bourg (ACRI), Philippe Goryl (ESA), Marc Bouvet (ESA)

Revisions:

Issue	Date	Subject	Author
1	20110527	Version 1.0	Doerffer


1 Overview

This document describes a procedure for the correction of the influence of the atmosphere and the specularly reflected solar radiation (sun glint) on radiance spectra measured with the Medium Resolution Imaging Spectrometer (MERIS). MERIS is part of the European Environmental Satellite ENVISAT of the European Space Agency ESA. It is used to determine water leaving radiance reflectances (RL_w) as input to the case 2 water algorithm in MEGS.

The fixed viewing geometry of imaging spectrometers for ocean colour observations such as MERIS or MODIS implies that part of the image is contaminated by specularly reflected solar radiation (sun glint), which makes the retrieval of the water leaving radiance difficult or impossible. Consequence is that part of the image, sometimes even half of the image, cannot be used for observing water constituents. The procedure as described in this ATBD allows to some extent also the correction of high sun glint.

The Atmospheric Correction is defined here as the determination of the water leaving radiance reflectance spectrum ($RL_w(\lambda)$) from the top-of-atmosphere radiance reflectance spectrum ($RL_{toa}(\lambda)$). It requires the determination of the radiance backscattered from all targets above the water surface including air molecules, aerosols, thin clouds, as well as all radiance, which is specularly reflected at the water surface, in particular the sun glint. Furthermore, the transmission of the solar radiance through the atmosphere to the water surface and of the radiance from the water surface to the sensor has to be computed.

The atmospheric correction procedure is based on radiative transfer simulations. The simulated radiance reflectances are used to train a neural network, which, in turn, is used for the parametrization of the relationship between the top of atmosphere radiance reflectances, RL_{toa} and the water leaving radiance reflectances (RL_w). Furthermore it computes (1) the atmospheric

 Helmholtz-Zentrum Geesthacht Centre for Materials and Coastal Research	DOC:	MERIS alternative atmospheric correction		
	DATE:	20110527		
	Issue:	1	Revision:	

path radiances (RL_path), (2) the downwelling irradiance at water level (Ed), (3) the aerosol optical thickness at 550 nm and three other wavelengths and (4) the angstrom exponents of the aerosol optical thickness. The water leaving radiance reflectances (RLw) is then be used as input to another procedure for retrieving the IOPs and concentrations of the water constituents.


The model atmosphere comprises three parts: (1) a standard atmosphere, which includes 50 layers with variable concentrations of different aerosols, cirrus cloud particles and a rough, wind dependent sea surface with specular reflectance, but with constant air pressure- and ozone profiles, (2) a layer on top of the standard atmosphere, which contains only the difference between the standard and real atmosphere concerning air molecules and ozone, and (3) a module to compute the water leaving radiance reflectance.

Three interfaces are defined: top of the actual atmosphere (TOA), top of standard atmosphere (TOSA) and bottom of atmosphere (BOA).

The atmospheric correction comprises three steps:

1. Calculation of the path radiances and transmittances of the variable "Rayleigh - ozone-layer" by using actual values of sea surface pressure and total ozone content from the ancillary data of MERIS and subtracting them from the standard values. Thus, the path radiance might become negative or the transmittance might become > 1 in cases where the air pressure and ozone content differences are negative. The path radiance and transmittances of this 'correction layer' are used to calculate the downwelling solar irradiance and the upward directed radiance at the top of standard atmosphere (TOSA). The actual pressure regards also the altitude of a lake by including the altitude-pressure formula into the procedure. Furthermore, the correction of a band shift along the cameras is performed in this module. This band shift is due to small misalignments of the 5 cameras. This has in particular an effect on the actual solar irradiance and the Rayleigh scattering. Both effects are corrected within this module.
Output of this procedure is the radiance reflectance at top of standard atmosphere, RL_tosa.
2. Calculation of the water leaving radiance reflectance, Rlw, by using a forward artificial neural network fwNN. The training of this network is based on the same training data set – computed with Hydrolight radiative transfer model -, which is used to train the backward NN for retrieving the inherent optical properties of water.
3. Calculation of the water leaving radiance reflectance, path radiances reflectance at TOSA, and the downwelling irradiance at bottom of atmosphere (BOA). This calculation is done with the neural network, which is trained with simulated radiances. It includes effects of different aerosols, cirrus clouds, specularly reflected sun and sky radiance and the coupling between all these components and the air molecules.

Input to the neural network are the TOSA radiance reflectances of 12 MERIS bands (412, 443, 490, 520, 560, 620, 665, 681, 708, 756, 778, 865 nm) as well as the solar zenith angle, the viewing zenith angles and the difference between viewing and sun azimuth angle. Output of the NN are the water leaving radiance reflectances, the path radiance reflectance and the downwelling irradiance, all of the 12 MERIS bands, and the aerosol optical thickness at 443, 550, 778, 865 nm from which the angstrom coefficient can be computed. Further outputs are the total scattering and absorption coefficients of water and the sun glint ratio. The core of the algorithm is a multiple non-linear regression method ("Neural Network", NN). Its coefficients are determined from a large set of simulated atmospheric and water conditions for the input variables and corresponding output variables. The coefficients of the NN are computed by using a feed forward back-propagation

 Helmholtz-Zentrum Geesthacht Centre for Materials and Coastal Research	DOC:	MERIS alternative atmospheric correction		
	DATE:	20110527		
	Issue:	1	Revision:	

optimisation ("training") technique. The data set for training and testing is produced by radiative transfer simulations using an ocean-atmosphere Monte Carlo photon tracing model, which has been developed at HZG. This model allows us to label the events, which a photons has encountered, By this it is possible to count photons separately as sun glint photons, which were specularly reflected at the surface and not scattered in the atmosphere.

In the MEGS processor all outputs of the NN are not used to generate products. Only the water leaving radiance reflectances are used as input to the NN, which determines the water IOPs.

2 Introduction

This ATBD describes the procedure to derive the bi-directional water leaving radiance reflectances (RL_w) from top of atmosphere (TOA) radiance reflectance spectra RL_toa (L1b data) of the *Medium Resolution Imaging Spectrometer* (MERIS) on ENVISAT. These reflectances are then used as input to the neural network system for determining water IOPs (absorption coefficient of phytoplankton pigment (a_pig), absorption coefficient of gelbstoff and bleached detritus (a_gd) and the scattering coefficient of the total suspended matter (b_tsm), all at MERIS band 2 (443 nm). A_pig is then converted into chlorophyll a concentration (product: algal_2) and b_tsm into total suspended matter dry weight concentration (product: total_susp). The a_gd value remains as an absorption coefficient. Its product name is yellow_subs.

The procedure is an alternative method to the standard atmospheric correction procedure for Meris. Its main purpose is to improve the atmospheric correction over turbid and highly absorbing case 2 water and for areas of an image, which are contaminated by sun glint. However, it is applied also to case 1 water for the products algal_2, total_susp and yellow_subs.


The procedure is mainly based on artificial neural networks with some pre-corrections. It delivers also information about spectra, which are out of the data set, which was simulated for training of the neural network and which determines the scope of the procedure. This value triggers the case 2 water quality flag. Furthermore, the path radiance reflectances (RL_path), the aerosol optical thicknesses and the angstrom coefficient are computed but used only as internal breakpoints.

Training of the neural networks is based on simulated bi-directional top of standard atmosphere radiance reflectances (RL_tosa). The simulations are performed for 12 bands of Meris. The radiative transfer model includes an atmosphere with 50 layers with different aerosols and thin cirrus clouds, a wind dependent rough sea surface with specular reflectance of sky and direct sun radiation and a water body with different components of absorbing and scattering constituents including a white scatterer for simulating the effect of white caps.

The procedure consists of four parts:

1. Determination of top of standard atmosphere (TOSA) spectra (RL_tosa) from RL_toa spectra
2. Check if spectrum is in range and in scope by an auto-associative NN (aaNN)
3. Determination of RL_w, RL_path by a NN (acNN)

Step 1 is used to perform a correction concerning the deviation of the actual surface pressure from the standard pressure of 1013.2 hPa. The correction of the deviation of the actual ozone column content from the standard value of 350 Dobson Units, and the correction for water vapour are done before by the standard procedure of the MEGS processor.

 Helmholtz-Zentrum Geesthacht Centre for Materials and Coastal Research	DOC:	MERIS alternative atmospheric correction		
	DATE:	20110527		
	Issue:	1	Revision:	

The general outline is summarized in Fig. 1

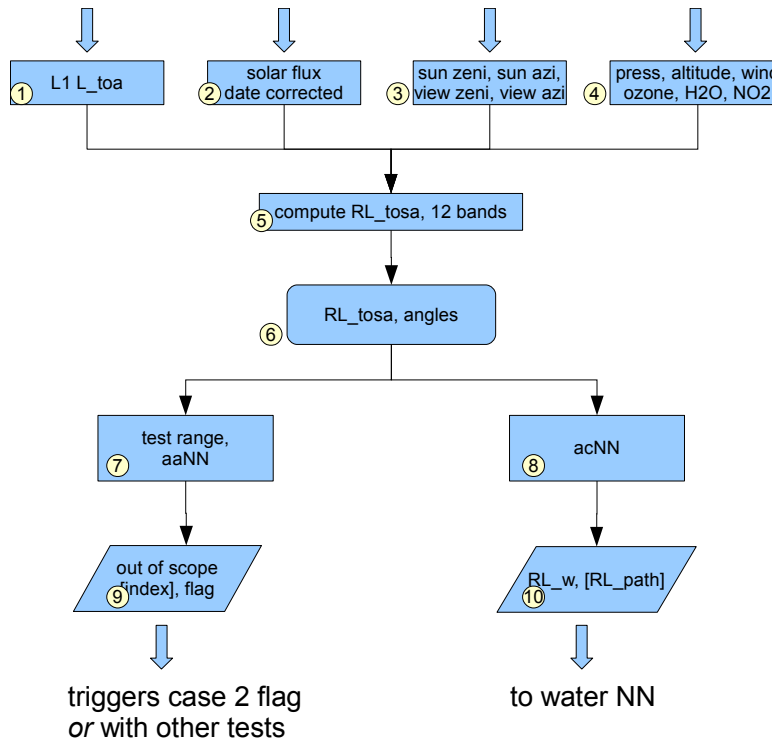


Fig. 1: Outline of atmospheric correction procedure

For the operation of the neural networks a routine to establish a NN and a routine to execute a network are necessary. These routines have to be consistent with the structure of the provided nn-files. Furthermore, a routine must be available to read the minimum and maximum values of the input neurons from the nn-file. These routines in the form of C-codes have been provided.

3 Input Data

3.1 MERIS data (1)

L1b top of atmosphere radiances in 12 bands:

3.2 Auxiliary data (2), (3), (4)

View zenith angle (at pixel location): view_zenith


View azimuth angle (at pixel location): view_azimuth

sun zenith angle (at pixel location): sun_zenith

sun azimuth angle (at pixel location): sun_azimuth

solar flux for day of overflight at top of atmosphere: E_0

air pressure at sea level: press_act

 Helmholtz-Zentrum Geesthacht Centre for Materials and Coastal Research	DOC:	MERIS alternative atmospheric correction		
	DATE:	20110527		
	Issue:	1	Revision:	

altitude of water surface (pressure correction for high lakes): alt

ozone column content in Dobson Unit: ozone_act

Water vapour column content: wv

4 RLtosa computation (5)

To keep the dimension of the simulated data for training of the neural network as small as possible the radiance reflectance at top of standard atmosphere, RL_tosa, is defined. This is used as input to the NNs. The top of standard atmosphere assumes standard values for pressure at sea level and for ozone and no influence by water vapour.

Thus, the following fixed standard values are used in the simulations for training of the NNs:

- pressure at sea level: press_std (1013.25 hPa)
- ozone: ozone_std (350 DU)
- no water vapour

The deviation between the actual and the standard values are used to compute RL_tosa from RL_toa, with

$$Ed_toa = E_0 * \cos(\text{sun_zenith})$$

$$RL_toa = L_toa / Ed_toa$$

$$L_tosa = L_toa * \text{trans_u_ozone} * \text{trans_u_raylc} * \text{trans_u_wv}$$

$$Ed_tosa = Ed_toa * \text{trans_d_ozone} * \text{trans_d_raylc} * \text{trans_d_wv}$$

$$RL_tosa = L_tosa / Ed_tosa$$

note: the transmittances can be > 1.0.

$$\text{trans_u_ozone} = \exp(-(\text{ozone_act_h} - \text{ozone_std}) * a_ozone / \cos(\text{view_zenith}))$$

$$\text{trans_d_ozone} = \exp(-(\text{ozone_act_h} - \text{ozone_std}) * a_ozone / \cos(\text{sun_zenith}))$$

$$\text{trans_u_raylc} = \exp(-(\text{press_act} - \text{press_std}) / \text{press_std} * b_rayl / 2 / \cos(\text{view_zenith}))$$

$$\text{trans_d_raylc} = \exp(-(\text{press_act} - \text{press_std}) / \text{press_std} * b_rayl / 2 / \cos(\text{sun_zenith}))$$


$$\text{trans_u_wv} = \exp(-wv * a_wv / \cos(\text{view_zenith}))$$

$$\text{trans_d_wv} = \exp(-wv * a_wv / \cos(\text{sun_zenith}))$$

The actual air pressure is calculated for the altitude of the water surface (press_act_h) to include also lakes in high altitudes as possible targets for Meris. To determine this pressure from the pressure at sea level the simple international barometric height formula for the standard atmosphere is used. The standard formula assumes a surface pressure of 1013.25 hPa, a temperature at surface of 15 deg C and a temperature gradient of 0.65 deg C per 100 meter.

$$p(h) = 1013,25 \left(1 - \frac{0,0065 \cdot h}{288,15} \right)^{5,255} \text{ hPa}$$

To calculate the pressure at water surface we use:

 Helmholtz-Zentrum Geesthacht Centre for Materials and Coastal Research	DOC:	MERIS alternative atmospheric correction		
	DATE:	20110527		
	Issue:	1	Revision:	

$press_act_h = press_act * (1 - 0.0065 * h / 288.15) ** 5.255$

with $press_act$ the actual pressure at sea level and h the altitude of the water level in meter.

b_rayl is the scattering coefficient of the standard atmospheric gases ("Rayleigh scattering") at standard pressure. Due to the forward-backward symmetry of the scattering function $b_rayl/2$ is taken as the diffuse attenuation coefficient.

a_ozone , and a_wv are the specific absorption coefficients for ozone and water vapour, i.e. per unit of column content.

Note: all above variables are wavelength dependent.

5 Angles

All angles are defined with respect to the position of the pixel. The viewing and sun azimuth angles are defined for the position of the sun and the satellite with the observer standing on the pixel with North 0 degree, East 90, South 180, and West 270 degree.

The azimuth difference is then:

$azi_diff = \text{absolute}(\text{view_azimuth} - \text{sun_azimuth})$

if ($azi_diff > 180$) $azi_diff = azi_diff - 180$

with respect to the definition of the simulated data:

$azi_diff = 180 - azi_diff$

The viewing angles are transformed into Cartesian coordinates:

$view_x = -\sin(\text{view_zenith}) * \cos(azi_diff)$

$view_y = \sin(\text{view_zenith}) * \sin(azi_diff)$

$view_z = \cos(\text{view_zenith})$


6 Out of range / scope computation / flags (7), (9)

The scope of the atmospheric correction network is determined by the training data set. Thus, it is checked whether a measured spectrum (RL_tosa) is within this scope.

First the input values are checked against the minimum/maximum values of each input of the networks. If any value is outside the range, the out_of_range flag will be raised. Since both networks are based on the same training data set, this test has to be performed only for one NN (i.e. the autoNN, (7)).

The minimum and maximum input values are included in the NN and are retrieved from there.

In a second step the type (form) of the RL_tosa spectrum is tested by using an auto-associative neural network. This NN tests if the input NN can be reproduced with an aaNN. The RMS difference between the input RL_tosa and the output RL_tosa' is used as an *out of scope index* and to raise a flag if the index is above a threshold. The aaNN is trained with the same training data set which is used for training of the acNN. Output neurons are the RL_tosa' values. The central hidden layer of this NN is used as bottle neck layer, i.e. the number of neurons is kept to a value, which is

 Helmholtz-Zentrum Geesthacht Centre for Materials and Coastal Research	DOC:	MERIS alternative atmospheric correction		
	DATE:	20110527		
	Issue:	1	Revision:	

just sufficient to reproduce RL_tosa' with a mean deviation of < 1% when using the simulated test data as input.

out_of_range_flag = if for any i_band (RL_tosa(i_band) > RL_tosa_max(i_band) OR
RL_tosa(i_band) < RL_tosa_min(i_band))

out_of_scope_index= sqrt(sum((RL_tosa'(i_band)-RL_tosa(i_band)/RL_tosa(i_band))**2))/n_band

out_of_scope_flag = if(out_of_scope_index > out_of_scope_threshold)

```

/* compute relative deviation (log of reflectance) as RMS error
for(i=0;i<12;i++)
    chi_sum += (((log(RL_tosa[i]) - outnet[i])/log(RL_tosa[i]))**2);
chi_sum = sqrt(chi_sum/12.0);

/* set flag as in MEGS 7.x pcd_16 */

chi_sum_max = THRESH_RL_TOSA_OOS;
if(chi_sum > chi_sum_max)
    *c2r_megs_flag |= PCD_16; // RL_tosa is out of scope of the nn, OR with pcd_16

```

Input to this aaNN (12x5x12_318.4.net) are:

sun_zenith angle (degree)

view_x

view_y

view_z

RL_tosa (12 bands)

Output of the aaNN are:

RL_tosa' (12 bands)

7 Computation of Water leaving radiance reflectance (8), (10)

The bi-directional water leaving radiance reflectances (RL_w) and path radiance reflectances (RL_path, only used for diagnostic purpose, not as product) are direct output of the acNN (8,10). RL_path includes the specularly reflected sun and sky light (fresnel reflection) and, thus, the sun glint. The output RL_w together with the 3 angles are used in the waterNN.

Input to this NN (20x25x45_55990.1.net) are:

sun_zenith angle (degree)

view_x

view_y


view_z

water temperature

water salinity

wind

RL_tosa (12 bands)

 Helmholtz-Zentrum Geesthacht Centre for Materials and Coastal Research	DOC:	MERIS alternative atmospheric correction		
	DATE:	20110527		
	Issue:	1	Revision:	

Output of this NN are:

RL_w (12 bands)

RL_path (12 bands)

7.1 Output variables

In total the atmospheric correction procedure provides the following variables as output:

- Top of atmosphere radiance reflectances: RL_toa (15 bands)
- Top of standard atmosphere radiance reflectances: RL_tosa (15 bands)
- Path radiance reflectances: RL_path (15bands)
- Water leaving radiance reflectances: RL_w (15 bands)
- Tau_aerosol_443
- Tau_aerosol_550
- Tau_aerosol_778
- Tau_aerosol_865
- angstrom coefficient
- out_of_range_flag
- out_of_scope_index
- out_of_scope_flag

7.2 The acNN

```
problem: D:\projekte\nn_hs\atmo_nn_20101103\simu_test_20090219_rlw_rlpath_20101103
saved at Thu Nov 4 17:44:48 2010
```

```
trainings sample has total sum of error^2=55990.129888
```


```
average of residues:
```

```
training 55990.129888/900092/16=0.001447 test 16819.002674/269908/43=0.001449
```

```
ratio avg.train/avg.test=0.998252
```

```
the net has 16 inputs:
```


```
input 1 is sun_zeni_deg in [1.020000,76.200000]
input 2 is x in [-0.707000,0.705600]
input 3 is y in [0.000002,0.707000]
input 4 is z in [0.707100,1.000000]
input 5 is log_rltosa_412 in [-3.281000,-1.409000]
input 6 is log_rltosa_443 in [-3.516000,-1.265000]
input 7 is log_rltosa_490 in [-3.890000,-1.120000]
input 8 is log_rltosa_510 in [-4.116000,-1.079000]
```


 Helmholtz-Zentrum Geesthacht Centre for Materials and Coastal Research	DOC:	MERIS alternative atmospheric correction		
	DATE:	20110527		
	Issue:	1	Revision:	

input 9 is log_rltosa_560 in [-4.515000,-1.022000]
input 10 is log_rltosa_620 in [-4.981000,-0.957300]
input 11 is log_rltosa_664 in [-5.217000,-0.877500]
input 12 is log_rltosa_680 in [-5.288000,-0.853800]
input 13 is log_rltosa_708 in [-5.441000,-0.819100]
input 14 is log_rltosa_753 in [-5.696000,-0.801000]
input 15 is log_rltosa_778 in [-5.838000,-0.785700]
input 16 is log_rltosa_865 in [-6.194000,-0.763600]

the net has 43 outputs:

output 1 is log_rlw_412 in [-9.672000,-2.368000]
output 2 is log_rlw_443 in [-9.210000,-2.330000]
output 3 is log_rlw_490 in [-8.473000,-2.388000]
output 4 is log_rlw_510 in [-8.184000,-2.622000]
output 5 is log_rlw_560 in [-7.599000,-2.870000]
output 6 is log_rlw_620 in [-9.076000,-3.184000]
output 7 is log_rlw_664 in [-9.764000,-3.301000]
output 8 is log_rlw_680 in [-9.851000,-3.335000]
output 9 is log_rlw_708 in [-10.630000,-3.598000]
output 10 is log_rlw_753 in [-11.870000,-4.511000]
output 11 is log_rlw_778 in [-12.140000,-4.710000]
output 12 is log_rlw_865 in [-13.010000,-5.337000]
output 13 is log_RLpath_412 in [-3.351000,-1.450000]
output 14 is log_RLpath_443 in [-3.563000,-1.293000]
output 15 is log_RLpath_490 in [-4.021000,-1.141000]
output 16 is log_RLpath_510 in [-4.247000,-1.104000]
output 17 is log_RLpath_560 in [-4.590000,-1.059000]
output 18 is log_RLpath_620 in [-5.000000,-0.987000]
output 19 is log_RLpath_664 in [-5.230000,-0.897000]
output 20 is log_RLpath_680 in [-5.302000,-0.870800]
output 21 is log_RLpath_708 in [-5.451000,-0.838600]
output 22 is log_RLpath_753 in [-5.700000,-0.807900]
output 23 is log_RLpath_778 in [-5.841000,-0.791200]
output 24 is log_RLpath_865 in [-6.197000,-0.766400]
output 25 is log_Ed_boa_412 in [-2.547000,-0.143900]
output 26 is log_Ed_boa_443 in [-2.471000,-0.110900]
output 27 is log_Ed_boa_490 in [-2.389000,-0.082300]
output 28 is log_Ed_boa_510 in [-2.376000,-0.077960]
output 29 is log_Ed_boa_560 in [-2.383000,-0.080130]
output 30 is log_Ed_boa_620 in [-2.303000,-0.066140]
output 31 is log_Ed_boa_664 in [-2.180000,-0.040820]
output 32 is log_Ed_boa_680 in [-2.129000,-0.032520]
output 33 is log_Ed_boa_708 in [-2.087000,-0.024290]

 Helmholtz-Zentrum Geesthacht Centre for Materials and Coastal Research	DOC:	MERIS alternative atmospheric correction		
	DATE:	20110527		
	Issue:	1	Revision:	

```

output 34 is log_Ed_boa_753 in [-2.040000,-0.017150]
output 35 is log_Ed_boa_778 in [-2.017000,-0.013090]
output 36 is log_Ed_boa_865 in [-1.966000,-0.008032]
output 37 is tau_443aero in [0.010000,0.948000]
output 38 is tau_550aero in [0.009472,0.610400]
output 39 is tau_778aero in [0.005020,0.602000]
output 40 is tau_865aero in [0.004660,0.601000]
output 41 is log_btot in [-4.381000,3.670000]
output 42 is log_atot in [-5.759000,2.457000]
output 43 is glintrat in [1.000000,107.700000]

```

8 Interface to further processing

The water leaving radiance reflectances (RL_w) together with the three angles (sun_zenith, view_zenith, azimuth_difference) are input to the waterNN.

9 Model for training of the neural networks

9.1 Introduction


The model consists of 3 parts, (1) the atmosphere for computing path radiances, transmittances, (2) the Fresnel reflectance at a rough, wind driven sea surface and (3) the water body for simulating a variability of water leaving radiances. All three parts are necessary to simulate realistic bi-directional radiance reflectances at top of atmosphere ($RL_{toa} = L_{toa}/Ed_{toa}$).

For this system a NN had to be trained, which is able to associate a measured top of atmosphere radiance reflectance with the corresponding water leaving radiance reflectance.

For this purpose, the model must comprise a large range of different constellations of case 1 and case 2 waters, of atmospheres with different aerosols and rough sea surfaces with sun glint. Furthermore, this range has to be defined properly and procedures have to be developed, which are able to detect and indicate measured spectra, which are out of this range and thus are out of scope of the algorithm.

Furthermore, different constellations must be uniformly distributed. Training of a NN is based on minimizing the deviation between the actual and the expected output of a neural network for a large number of samples. Thus, constellations of variables, which are under represented in the training data set, implicitly have a minor weight and the NN will be less accurate for these constellations. The problem is, that in a multi-component system a uniform distribution of each component, e.g. extinction coefficients of different aerosols or water constituents, lead to a Gaussian distribution of the total extinction coefficient. Consequence is that the trained NN will perform better around the maximum of the Gaussian distribution than at the sides.

To avoid such a bias, the frequency distribution of each component has to be defined in a way that also the overall properties are uniformly distributed as much as possible over the full required range.

 Helmholtz-Zentrum Geesthacht Centre for Materials and Coastal Research	DOC:	MERIS alternative atmospheric correction		
	DATE:	20110527		
	Issue:	1	Revision:	

9.2 Model of the atmosphere

Aerosols

The properties of the aerosols, which are used in the simulations and which define the scope of the algorithm, are adopted from WCRP 112 (1986), Shettle & Fenn (1979), from the MERIS atmospheric correction ATBD (Antoine & Morel, 1999) and from the Mie program of the Institute for Space Science, FUB Berlin (Heinemann & Schüller, 1995).

According to the recommendations of WCRP112, aerosols are constructed from basic aerosol components, which consists of spherical particles with a log-normal or a modified gamma size frequency distribution. Properties of these components are given in table 1.

According to Shettle & Fenn (1979) the refractive index of some of the aerosols depends strongly on the relative humidity. Thus, their optical properties have been defined as given in table 1.

From these basic components different aerosol models have been defined as described in WCRP 112, those 4, which are used in this ATBD, are:

1. The continental (background) aerosol consists of 70% of dust-like particle, 29% of water soluble and by 1% of soot.
2. The maritime model consists of 95% of oceanic component and a 5% fraction of water-soluble. The refractive index depends on the relative humidity (RH), for the simulation an RH of 99 % has been used to get a white aerosol component in the boundary layer.
3. Urban / Industrial aerosol model consists of 17% of dust-like particle, 61% of water soluble and by 22% of soot, two RHs with 45% and 95%.
4. The stratospheric aerosol is a 75% solution of sulfuric acid in water.

aerosol component	refr.index real (550)	refr. Index imag.	Dr0	rb	P1	P2	rmax	step	
water sol.	1.530	0.600E-02	1	0.500E-02	2.990	0.00	0.00	20.0	0.002
dust-like	1.530	0.800E-02	1	0.500E-00	2.990	0.00	0.00	40.0	0.020
soot	1.750	0.440E-00	1	0.118E-01	2.000	0.00	0.00	30.0	0.005
h2so4	1.430	1.000E-08	3	0.324E-03	18.00	1.00	1.00	4.8	0.001
oceanic	1.381	0.426E-08	1	0.300E-00	2.510	0.00	0.00	40.0	0.020

Table 1 Basic standard aerosol components, as defined in WCRP112 (1986) and Heinemann & Schüller(1995) and used for Mie calculations

However, in order to achieve the wide range of angstrom coefficients between 0.1 and 2.0, as required for ocean and coastal areas and as measured at coastal AERONET stations, the composition and Mie calculations had to be slightly changed.

One change regards the size distribution. A logarithmic scaling was introduced into the Mie calculation instead of a linear scale in order to get a better representation of the small particles (Table 2, Figure 2). The effect was that the angstrom coefficients, computed by using the

attenuation coefficients at 440 and 870 nm of these components changed according to Table 2.

Component	Angstrom coefficient with linear size distribution	Angstrom coefficient with logarithmic size distribution
Water sol.	-1.297	-2.721
Dust-like	0.0615	0.0765
Soot	-1.394	-1.368
Oceanic	0.0924	-0.113
H2SO4	-1.508	-1.852

Table 2: Change in angstrom coefficient from linear to logarithmic size distribution. Angstrom coefficient is computed from the attenuation coefficients at 440 and 870 nm

Furthermore the compositions for the maritime and urban aerosol was changed according to Table 4.

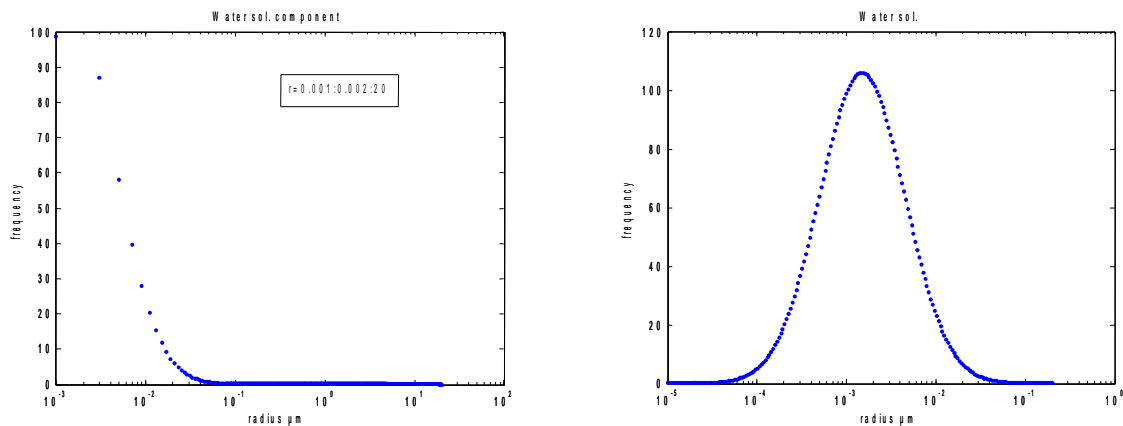



Fig. 2: Computation of the particle size frequency distribution for the water soluble component with a linear (left) and logarithmic (right) distribution

 Helmholtz-Zentrum Geesthacht Centre for Materials and Coastal Research	DOC:	MERIS alternative atmospheric correction		
	DATE:	20110527		
	Issue:	1	Revision:	

```

output-file: mwanglc.sex          (09) mqco = optical properties
              mwanglc.pfu        (10) mpco = phase-function
No. name(10char) wavel.  RFR      RFI  Typ  r0      rb      P3  P4  rmax  nstep  rmin
101 water sol.  0.5500  1.530  0.600E-02  1  0.500E-02  2.990  0.00  0.00  0.2  500  0.00001
102 dust-like  0.5500  1.530  0.800E-02  1  0.500E-00  2.990  0.00  0.00  10.0 500  0.00200
103 soot       0.5500  1.750  0.440E-00  1  0.118E-01  2.000  0.00  0.00  0.2  500  0.00050
104 oceanic    0.5500  1.381  0.426E-08  1  0.300E-00  2.510  0.00  0.00  5.0  500  0.00200
106 rural99    0.5500  1.000  0.111E-00  1  5.215E-02  2.239  0.00  0.00  1.0  500  0.00050
107 urban50    0.5500  1.000  0.111E-00  1  2.563E-02  2.239  0.00  0.00  1.0  500  0.00050
190 h2so4      0.5500  1.430  1.000E-08  3  0.324E-03  18.00  1.00  1.00  2.0  500  0.00005
  0  ENDE      0.0000  0.000  0.000E+00  0  0.000E-00  0.000  0.00  0.00  0.0  000  0.00000

  4  Spektrum
meris_lam_nomi_20051023.txt
101 rfi/watsol.rfi
102 rfi/dust.rfi
103 rfi/soot.rfi
104 rfi/oceanic.rfi
106 rfi/sflr99.rfi
107 rfi/sfsu50.rfi
190 rfi/h2so4.rfi
123456789-123456789-123456789-123456789-123456789-123456789-123456789

```

Table 3: Properties of aerosol components as used for the Mie calculations with size distribution on logarithmic scale

No.	Component s. table 2	Relative density of particles for Maritime aerosol component	Relative density of particles for urban aerosol component
1	101	0.00	0.999
2	104	0.99	0.001
3	106	0.01	0.000

Table 4: Composition of maritime and urban aerosol as used in the Mie calculations

The attenuation spectra of the two boundary layer aerosols can be seen in Fig. 3, the phase functions in Fig. 4 and 5 and the range of the angstrom coefficients and optical thicknesses over all aerosols is given in Fig. 6.

DOC:	MERIS alternative atmospheric correction		
DATE:	20110527		
Issue:	1	Revision:	Page: 14 of 27

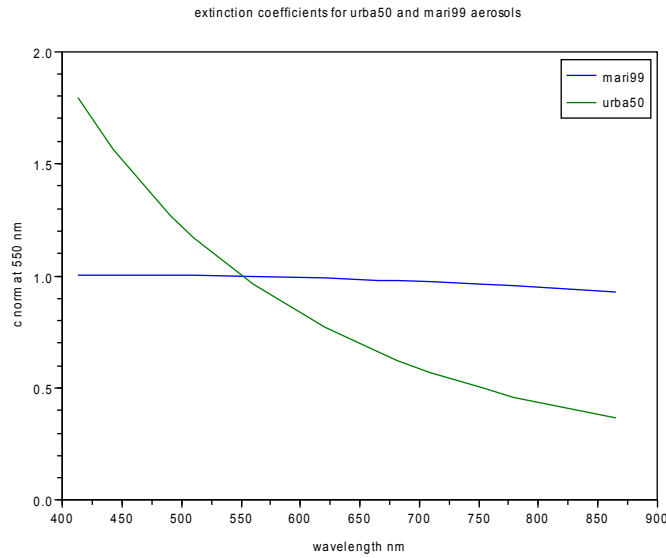


Fig. 3: attenuations coefficients of maritime and urban aerosols, normalized at 550 nm. The maritime aerosol has an angstrom coefficient of -0.065 , the urban aerosol of -2.15

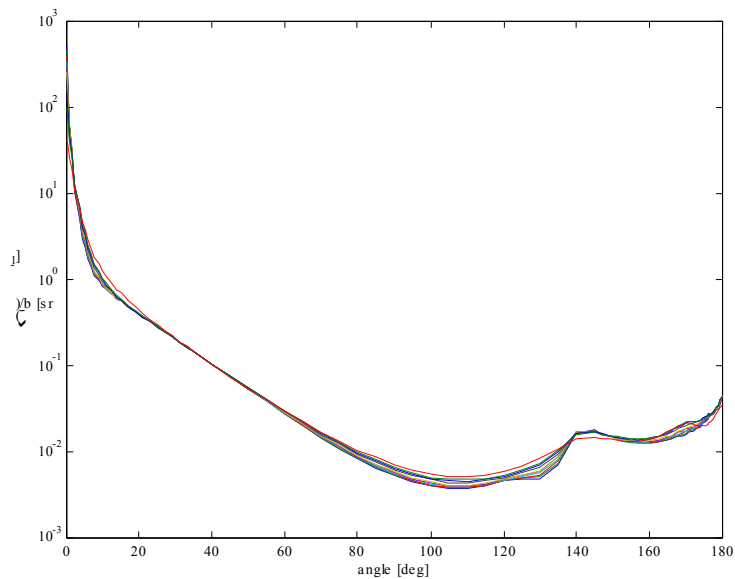



Fig. 4 Phase function of maritime aerosol of 99% humidity for wavelength range 408 - 900 nm

 Helmholtz-Zentrum Geesthacht Centre for Materials and Coastal Research	DOC:	MERIS alternative atmospheric correction		
	DATE:	20110527		
	Issue:	1	Revision:	

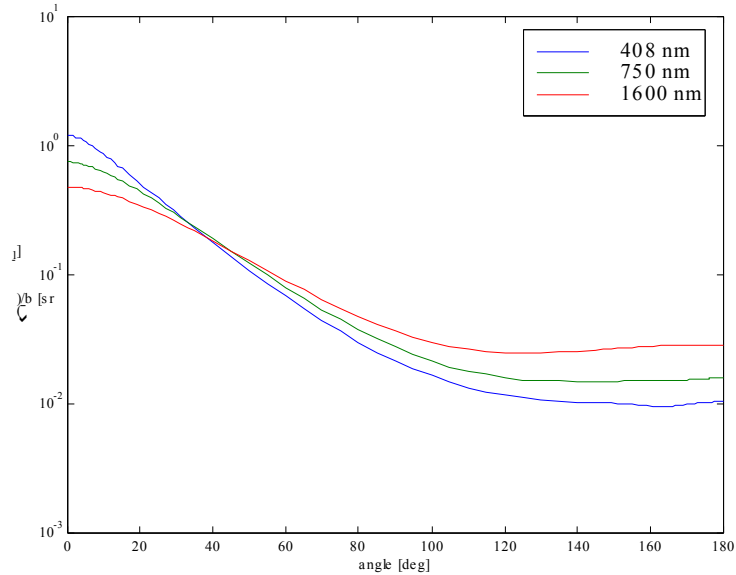


Fig. 5 Phase function of urban aerosol (50% humidity)

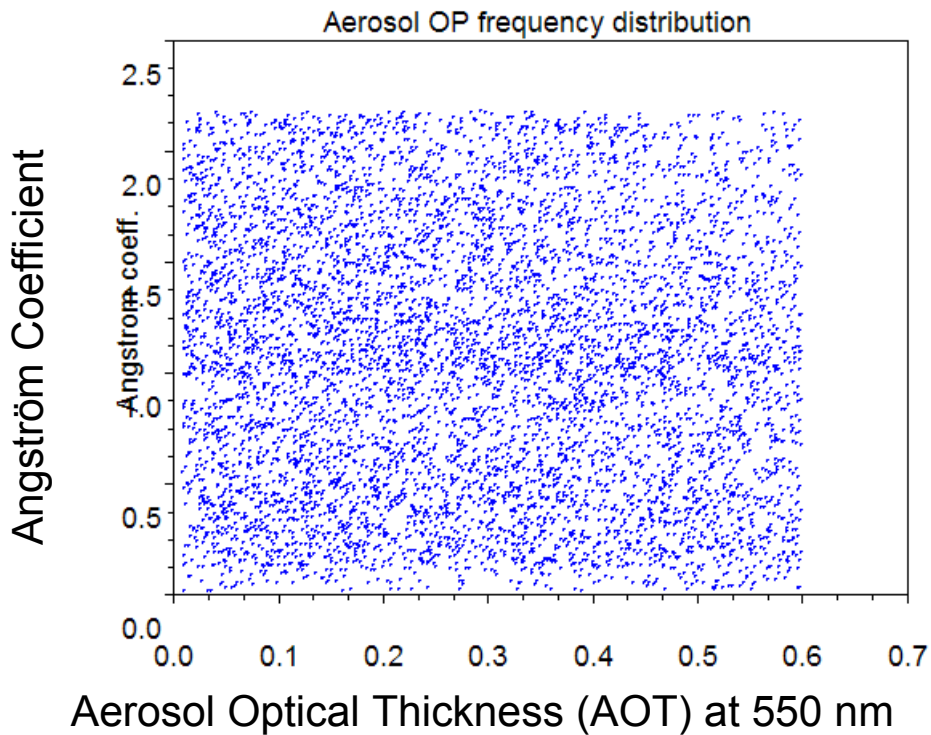



Fig. 6: Scatter plot of the distribution of aerosol optical thickness and angstrom coefficient

For creating the uniform distribution of optical thickness and angstrom coefficient over the full range of aerosol optical properties during the simulation runs the aerosol concentrations were

 Helmholtz-Zentrum Geesthacht Centre for Materials and Coastal Research	DOC:	MERIS alternative atmospheric correction		
	DATE:	20110527		
	Issue:	1	Revision:	

selected according to the following scheme:

First a total attenuation value is randomly selected from an uniform distribution between 0 and maximum of the total aerosol optical thickness. Then from this value optical thicknesses are selected for each component in a loop until the pre-selected total attenuation is reached. By this selection scheme the overall optical thickness and angstrom coefficient were nearly uniformly distributed (Fig. 6).

Cirrus

For simulation of cirrus clouds the scattering function of cirrus ice crystals derived from ray-tracing simulations with fractal-shaped crystals have been adapted from Macke et al. (1996). Because of the large size of the cirrus particles a flat spectral scattering is assumed. The phase function is presented in Fig. 7

The mean cirrus altitude and geometrical thickness is defined according to statistical parameters from a one year lidar monitoring at LMD (geog. position at 48 N, 02 E) during CIRREX'93 (Elouragini et al., 2005), s. Table 5.

Cirrus parameter	Daily average minimum	Daily average maximum	Yearly average	Standard deviation	Normalized standard deviation
base (km)	5.0	11.0	8.0	1.7	0.21
top (km)	8.0	13.0	10.8	1.3	0.12
geometrical thickness (km)	0.5	6.0	2.8	1.5	0.54
extinction coefficient (m ⁻¹)	0.010	0.42	0.079	0.046	0.58
backscattering coefficient	0.001	0.025	0.0047	0.0027	0.57
optical depth	0.1	1.2	0.25	0.15	0.6

Table 5 Parameters of statistical distributions for cirrus altitude, geometrical thickness, and optical parameters at 530 nm as recorded during CIRREX'93.

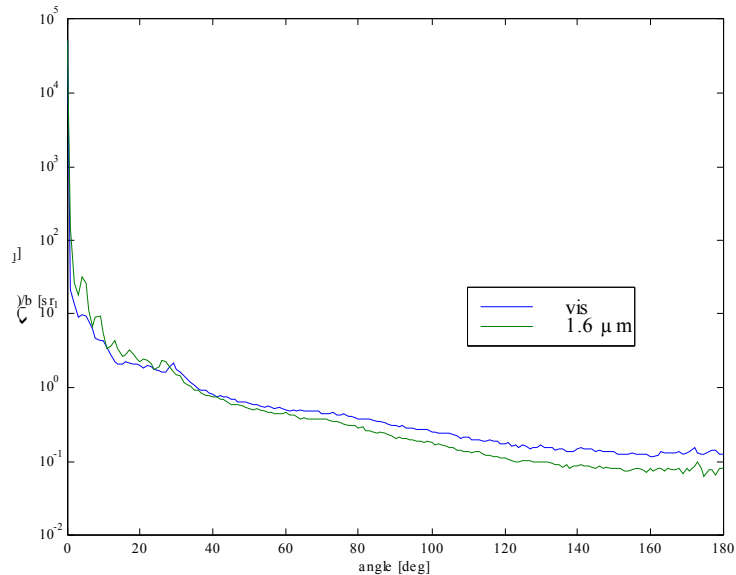



Fig. 7 Phase function cirrus ice particles (data from Macke et al., 1996)

Specular reflection at the sea surface

The specular reflection at the sea surface is computed by using the Fresnel reflection formula with the spectral refractive index of sea water for a temperature of 15 deg C as provided by Austin & Halikas (1976) and confirmed by IAPWS (1997) and listed in the MERIS reference model. The surface slopes of the waves are computed as a function of the wind speed using the formulation of Cox&Munk (1954).

Lam (nm)	n
412.5	1.349
442.5	1.347
490.0	1.344
510.0	1.343
560.0	1.341
620.0	1.339
665.0	1.338
681.25	1.338
708.75	1.337
778.75	1.336
865.0	1.334

Refractive index of sea water (salinity 35, temperature 15 deg C)

 Helmholtz-Zentrum Geesthacht Centre for Materials and Coastal Research	DOC:	MERIS alternative atmospheric correction		
	DATE:	20110527		
	Issue:	1	Revision:	

Water leaving radiance

The water leaving radiance is computed by using a forward neural network, which has been trained with simulated bi-directional RL_w spectra. Its input are:

- sun zenith angle: sun_zeni_deg in [1.800000,82.300000] deg
- viewing zenith angle: view_zeni_deg in [0.000000,46.340000] deg
- difference between viewing and sun azimuth: azi_diff_deg in [0.000000,180.000000] deg
- absorption coefficient of particles: log_apart in [-9.104000,1.631000] (0.0001- 5.1 m-1)
- absorption coefficient of yellow substance: log_agelb in [-5.298000,1.608000] (0.005 - 5.0 m-1)
- absorption coefficient of phytoplankton pigment: log_apig in [-6.908000,1.385000] (0.001 - 4.0 m-1)
- scattering coefficient of particles: log_bpart in [-5.297000,3.399000] (0.005 – 30.0 m-1)
- scattering coefficient of white particles: log_bwit in [-5.298000,3.401000] (0.005 – 30.0 m-1)

All coefficients are for MERIS band 2 (443 nm). Output are the water leaving radiances at 12 MERIS bands.

9.3 Vertical distribution and concentration ranges

The atmosphere model (Fig. 8) is separated in two parts: Part 1 contains the variable aerosol / cirrus concentrations with a constant Rayleigh scattering and ozone absorption profile. It has 50 layers, each 1 km thick. Part 2 consists of 2 virtual layers on top of this standard atmosphere with only a variable ozone and Rayleigh scattering atmosphere. These two second layers are used to correct for the deviations of these two quantities from the standard profile of part 1, where they have a profile with constant concentrations. The correction values may get negative radiances or transmittances > 1. The deviations are computed as the difference between the standard values and the ozone content and surface pressure are taken from the MERIS standard L1 product (s. chapter 4).

Model Atmosphere

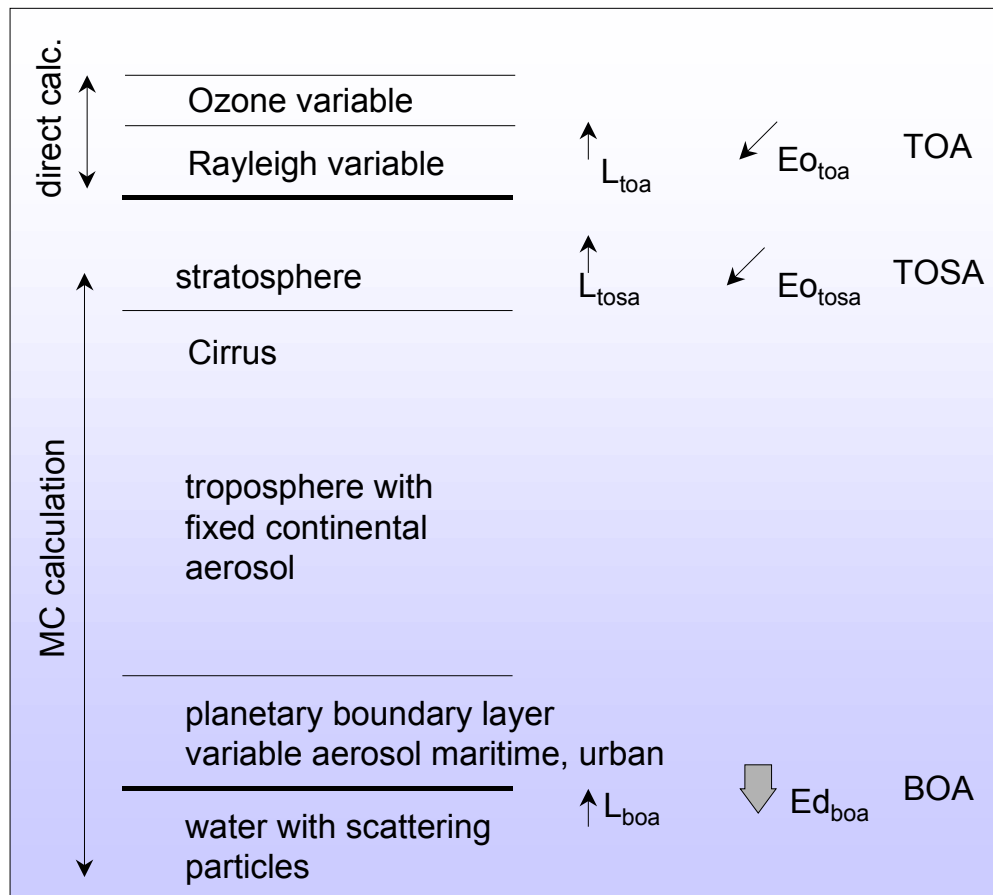



Fig. 8 Model atmosphere, TOA is top of atmosphere, TOSA top of standard atmosphere and BOA is bottom of atmosphere

Rayleigh scattering

The vertical profile of the Rayleigh scattering coefficient is given by Elterman(1968) for the standard atmospheric pressure of 1013.25 hPa at sea level (Fig. 9). The profiles with 50 1 km-layers are tabulated for each MERIS band. The profile for the simulation of the TOA radiance reflectances for the training data set is fixed. The deviation of the radiances and transmittances from the standard pressure is computed separately and used to compute the radiance reflectance at top of the standard atmosphere (RL_toa). In case of lakes this deviation includes also the altitude of the water.

Ozone absorption

The vertical ozone profile is taken from Elterman(1968), Fig. 9. The density profile is given in cm ozone per km for a surface pressure of 1013.25 hPa. The total ozone column content is 0.35 cm. The extinction profiles with 50 1-km-layers are tabulated for each MERIS band. Also the ozone profile is fixed for the simulation of the training data set. Deviations from the standard concentration of 350 Dobson units (DU) are computed in a separate module (s. chapter 4).

 Helmholtz-Zentrum Geesthacht Centre for Materials and Coastal Research	DOC:	MERIS alternative atmospheric correction		
	DATE:	20110527		
	Issue:	1	Revision:	

Aerosols and Cirrus

Each of the 4 aerosol and cirrus has a predefined vertical profile within the model atmosphere of 50 layers with maximum concentrations for each layer (Fig. 8 and 10, Table 6). During the simulation run the concentration profile for each aerosol / cirrus component is modified by a randomly selected factor in the range 0 and 1. In the extreme minimum case the whole atmosphere consists only of Rayleigh scattering and ozone absorption.

The aerosol / cirrus optical thicknesses for this model atmosphere are given in table 6 and the profiles of the maximum values are given in Fig.6.2.8

As one can see from this table, the dominating effects come from the urban aerosol, the maritime aerosol and the cirrus clouds.

The aerosol properties have been chosen according to AERONET measurements at coastal stations (Behnert et al., 2007).

Aerosol	Layer [km]	Optical thickness at 550 nm	Max mean Extinction at 550 nm [km⁻¹]
maritime (99 % rel. hum.)	0 - 2 km	0 - 0.2	0.1
urban (45% rel. hum.)	0 - 2 km	0 - 0.5	0.25
continental	2-12	0 - 0.165	0.0165
cirrus	8-11	0 - 0.3	0.1
stratosphere	12-50	0 - 0.003	0.0000625
max. optical thickness		1.168	

Table 6: Ranges of optical thicknesses of aerosols and cirrus clouds

DOC:	MERIS alternative atmospheric correction		
DATE:	20110527		
Issue:	1	Revision:	
			Page: 21 of 27

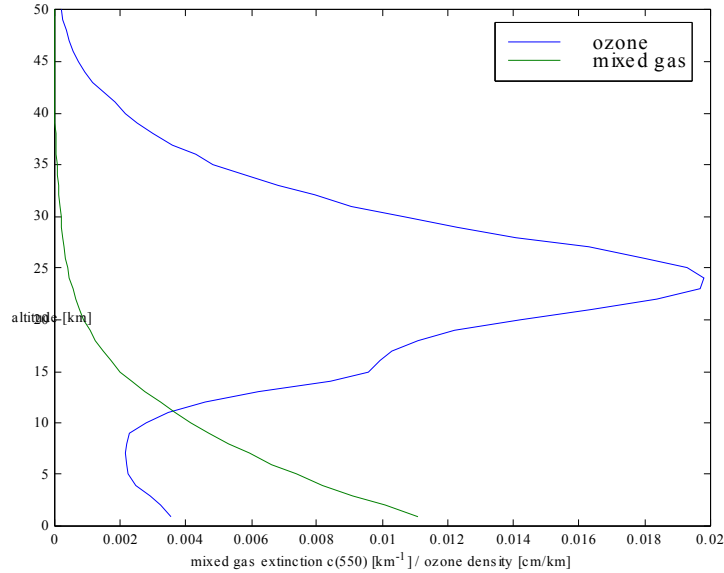


Fig. 9 Mixed gas extinction (550 nm) and ozone density profile

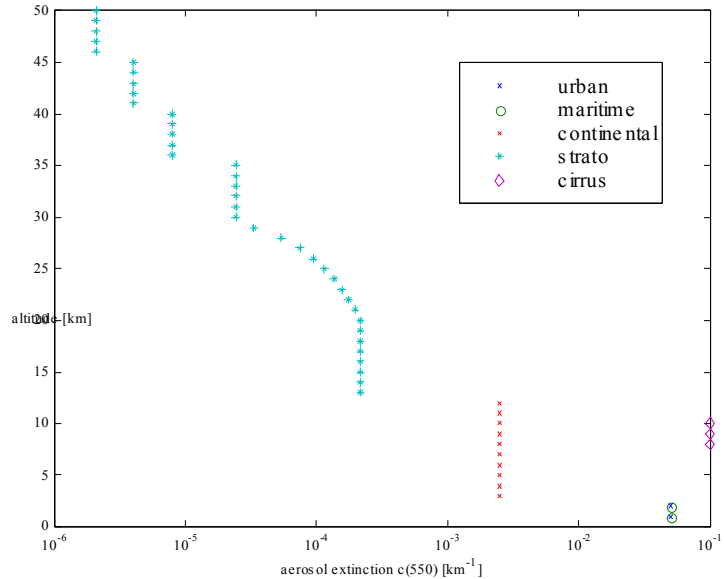



Fig. 10 Vertical profile of extinction at 550 nm for different aerosols

10 Radiative transfer simulations

For the simulations an angular resolving ocean-atmosphere photon tracing Monte Carlo radiative transfer code is used. It has been developed by GKSS (HZG) and is partly based on publications by Gordon (1997), Mobley(1994), Morel & Gentili (1991).

In its realisation for this application it has the following features:

 Helmholtz-Zentrum Geesthacht Centre for Materials and Coastal Research	DOC:	MERIS alternative atmospheric correction		
	DATE:	20110527		
	Issue:	1	Revision:	

- atmosphere with 50 layers using vertical profiles for Rayleigh scattering, ozone absorption and scattering and absorption of five different aerosols.
- air/sea interface with flat or wind dependent rough sea surface (2)
- unstratified water column
- bottom at a depth with no effect on water leaving radiance

Processes which are not included in the simulation are:

- polarization
- any inelastic scattering (fluorescence, Raman scattering)
- wind direction
- computation of the water leaving radiance

The detectors are positioned just above the water surface for counting the downwelling irradiance and at top of the standard atmosphere to determine the TOSA radiance reflectance for different viewing and solar angles. The angular distribution of radiance is resolved with an angle of 7.5 degrees in azimuth and zenith distance.

Photons start with a weight of 1 for all wavelengths at top of atmosphere (layer 51 of the model atmosphere) from a sun disc of 0.5 degree apparent diameter. The weight is multiplied with the cosine of the sun zenith angle to get the downwelling irradiance E_{d_toa} . At each collision event the photon weight is multiplied with the single scattering albedo, ω_0 , of the layer in which the event happens, to take into account for the probability of absorption. The travel distance between two collision events is calculated from a random pull. When the weight is reduced to a value of < 0.01 a "Russian Roulette" decision procedure is started to either end the life of the photon or increase the weight again.


The type of scattering is determined from the concentration mixture of the different media or constituents in water or air. Probability tables for the random pull of the type of scattering are pre-generated for each layer. The scattering angle at each event is randomly pulled from large tables which contain, for each media or constituent, the pre-calculated probabilities for the scattering angle in theta.

The weights of photons, which reach the air/sea interface layer in downwelling direction, are counted for calculating the downwelling vector irradiance.

The wave slope angles are randomly pulled from a probability table, which is calculated using the Cox & Munk (1954) wind dependent sea surface slope distribution. This distribution is isotropic with respect to the azimuth, i.e. it does not take into account the wind direction.

The simulation for one case and one wavelength is completed when a predefined number of photons have reached the radiance detector, i.e. the number of started photons is variable in order to account for strong differences in ω_0 of different concentrations mixtures and wavelengths. The standard deviation from this photon counting is also recorded. Furthermore, all sun glint photons are labelled and counted separately. They are defined as those photons, which were never scattered in the atmosphere.

Result of the MC simulation are the top of standard atmosphere radiance reflectance, the path radiance reflectance, the sun glint, the downwelling irradiance at bottom of atmosphere and the optical thicknesses for the total and the individual aerosols. Glint and no-glint photons are summed up to get the total path radiance.

 Helmholtz-Zentrum Geesthacht Centre for Materials and Coastal Research	DOC:	MERIS alternative atmospheric correction		
	DATE:	20110527		
	Issue:	1	Revision:	

To compute the total radiance reflectance at top of standard atmosphere RL_{tosa} , the water leaving radiances RL_w has to be added to the path radiance reflectances RL_{path} after its transmittance through the atmosphere t_{rlw} .

$$RL_{tosa} = RL_{path} + t_{rlw} * RL_w$$

Although the MC code allows to include the computation of RL_w , by allowing the photons to dive into the water, this feature was not used because of its high computational time requirement. Instead the forward NN of the water retrieval was used to simulate RL_w . It is based on a water bio-optical model, which is determined by generic optical components. This separation of the atmospheric from the water part allows a much higher flexibility and efficiency for generating training data sets for different water conditions. A further step is the computation of the transmittance of RL_w to TOSA. Now all values are computed for the full range of variables. However since it is unlikely or impossible that a NN can handle and produce acceptable results for all of these possible cases, a selection is performed for the training of different NN. In particular it is necessary to restrict the maximum sun glint contribution and the maximum aerosol optical thickness for cases with highly absorbing water, i.e. with high concentrations of yellow substances and phytoplankton pigments, so that the final training data set is only a subset of the total.


MERIS band No.	central wavelength	used for AC
1	412	x
2	443	x
3	490	x
4	510	x
5	560	x
6	620	x
7	665	x
8	681	x
9	708	x
10	753	x
11	760	
12	778	x
13	865	x
14	885	
15	900	

Table 6 MERIS bands used for atmospheric correction

11 Training of the neural network

Main Task of the neural network is to establish the relationship between the radiance reflectances at top of standard atmosphere (TOSA) with the water leaving radiance reflectance of the 12 MERIS bands. After the conversion $RL_{toa} \rightarrow RL_{tosa}$, RL_{tosa} can be used as input to the NN, which provides then the requested RL_w as output.

For training of such a network, i.e. for determining all coefficients of the NN, a training data set has

 Helmholtz-Zentrum Geesthacht Centre for Materials and Coastal Research	DOC:	MERIS alternative atmospheric correction		
	DATE:	20110527		
	Issue:	1	Revision:	

to be computed, which consists of pairs of input and output variables. Depending on the range of environmental conditions, which determine the input and output variables, the number of cases has to be sufficient large ($\gg 100\,000$ cases) to ensure a high interpolation capability of the NN. Thus, a Linux cluster is used to perform the radiative transfer calculations in acceptable time.

The range of environmental conditions is determined in our case by the optical thicknesses of the 4 aerosol types, cirrus optical thickness, sun glint and the water leaving radiances, which in turn depends on the optical properties and concentrations of water constituents. This range determines also the scope of the algorithm.

In the case of the NN, which we have designed, also the path radiance reflectance, the transmittance and the aerosol optical thickness have been included in the training and are outputs of the NN. Furthermore the glint ratio and the total absorption and scattering of water are included as control outputs.

The outline of the NN is given in Fig. 11.

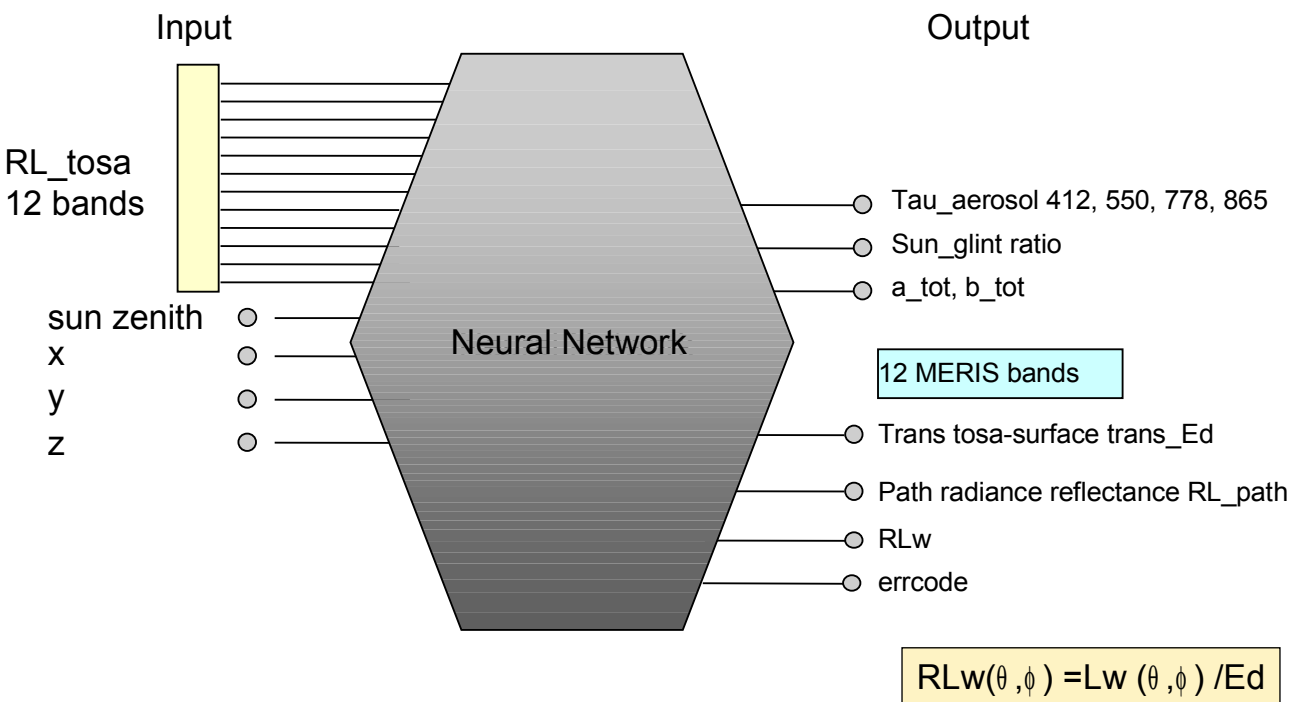



Fig. 11: Outline of the neural network to determine the water leaving radiance reflectance RL_w

11.1 The training of the atmospheric correction NN

The Monte Carlo model was used to calculate the top of standard atmosphere path radiance reflectances and the downwelling irradiance at sea level. The ranges of interest of the variables were defined to be those given in Table 6. The values were chosen to cover a large range of ocean, coastal and land aerosols and cirrus clouds. However, different trials demonstrated that it was necessary to limit e.g. the maximum optical thickness and sun glint to values, where the water leaving radiance reflectance is still detectable within the RL_tosa spectrum. For the $25 \times 30 \times 40_5365.2.net$ NN the maximum aerosol optical thickness at 550 nm was set to 0.3 and the maximum sun glint ratio to 6.0, range of water leaving radiance reflectance at 560 nm to 0.0005 –

 Helmholtz-Zentrum Geesthacht Centre for Materials and Coastal Research	DOC:	MERIS alternative atmospheric correction		
	DATE:	20110527		
	Issue:	1	Revision:	


0.04, and for 620 nm a maximum of 0.04. Range for 412 nm was restricted to 0.0001 – 0.03.

First 15000 cases of path radiances and irradiances were computed with randomly selected sun zenith distances, wind speeds and sun glint, aerosols and cirrus clouds. For each case 7 viewing angles were randomly selected. Then for each of these 105 000 cases 10 different water leaving radiances were added, which were also randomly computed as described above. From the resulting 1 Mio spectra the selection was made with respect to maxima values of sun glint, reflectance ranges and tau550 of aerosols to build the final training data set. About 66% of these data are used for training, the other 34 % are used for testing during the training process in order to avoid overtraining. Thus it is constantly checked that the error of the training data set is similar to that of the test data set.

The software which was used for training the NN is the GKSS Neural Network Simulator FFBP v1.0 (Schiller, 1997). The NN is fully connected (each 'neurone' of a layer is connected with each 'neuron' of the following layer) and is initialised by assigning random numbers (uniformly in (0,1)) to the weights and biases.


For error-minimisation the backpropagation method with momentum and flat spot term was used. The 'teaching'-sample was applied to the ffNN in random order. At start the control parameters were set as follows: learning factor 0.6, momentum factor 0.2 and flat spot term 0.02. Each time if the error-function did not decrease any more the minimisation-parameters were divided by 3. The minimisation was continued until the error function was down to an average output error of 1%.

The weights and biases obtained by 'teaching' of the ffNN were used to generate a table including parameters of the architecture of the NN and all coefficients. An interface routine reads this table and constructs the network in a preparatory set-up step before using the net pixel by pixel. Also the backtransformation from the (0,1)-interval for the components are built into this function.

 Helmholtz-Zentrum Geesthacht Centre for Materials and Coastal Research	DOC:	MERIS alternative atmospheric correction		
	DATE:	20110527		
	Issue:	1	Revision:	

12 References

- André, J.M. and A. Morel (1989). Simulated effects of barometric pressure and ozone content upon the estimate of marine phytoplankton from space, *Journal of Geophysical Research*, 94, 1029-1037.
- André, J.M. and A. Morel (1991). Atmospheric corrections and interpretation of marine radiances in CZCS imagery, revisited, *Oceanologica Acta*, 14, 3-22.
- Ångström, A (1964): The parameters of atmospheric turbidity, *Tellus*, 26, 64-75
- Antoine, D. and Morel, A., 1998, Relative importance of multiple scattering by air molecules and aerosols in forming the atmospheric path radiance in the visible and near-infrared parts of the spectrum, *Applied Optics*, 37, 2245-2259.
- Antoine, D. and A. Morel (1999). A multiple scattering algorithm for atmospheric correction of remotely-sensed ocean colour (MERIS instrument) : principle and implementation for atmospheres carrying various aerosols including absorbing ones, *International Journal of Remote Sensing*, 20, 1875-1916.
- Austin, R.W. and G. Halikas, 1976. The index of refraction of seawater, SIO Ref. No. 76-1, Scripps Inst. Oceanogr., La Jolla, 121 pp.
- Behnert, Irina, Matthias, Volker, Doerffer, Roland (2007): Aerosol climatology from ground-based measurements for the southern North Sea, *Atmospheric Res.*, 2007
- Cox, C., and W. Munk (1954): Statistics of the sea surface derived from Sun glitter. *Journal of Marine Research*, 13, 198-227
- Doerffer R, Fischer J (1994) Concentrations of chlorophyll, suspended matter, and gelbstoff in case II waters derived from satellite coastal zone color scanner data with inverse modeling methods. *Journal Geophysical Research* 99:7457-7466
- Doerffer, R. and H. Schiller (2007): The MERIS Case 2 water algorithm, *International Journal of Remote Sensing*, Vol. 28, Nos. 3-4, 2007, pp 517-535, 2007.
- Eltermann, L. (1968): UV, visible, and IR attenuation for altitudes to 50 km. *Environmental Research Paper No. 285, AFCRL-68-0153, Airforce Cambridge Research Laboratories*
- Elouraginia, Salem, Houda Chtiouia, and Pierre H. Flamant (2005): Lidar remote sounding of cirrus clouds and comparison of simulated fluxes with surface and METEOSAT observations, *Atmospheric Research*, Volume 73, Issues 1-2, January 2005, Pages 23-36
- Gordon, H.R., and A. Morel (1983). Remote assessment of ocean color for interpretation of satellite visible imagery. A review, Springer-Verlag, New York (USA).
- Gordon, H.R. : Atmospheric Correction of Ocean Color Imagery in the Earth Observing System Era, *Jour. Geophys. Res.*, 102D, 17081-17106 (1997).
- Heinemann, Thomas and Lothar Schüller (1995): MIE-Programmpaket für Strahlungstransportsimulationen mit MOMO, Institut für Weltraumwissenschaften, Freie Universität Berlin
- IAPWS (1997): Release on the Refractive Index of Ordinary Water Substance as a Function of Wavelength, Temperature and Pressure, The International Association for the Properties of Water and Steam, Erlangen, Germany, September 1997

 Helmholtz-Zentrum Geesthacht Centre for Materials and Coastal Research	DOC:	MERIS alternative atmospheric correction		
	DATE:	20110527		
	Issue:	1	Revision:	

Krasnopolsky, V. and H. Schiller (2003): Some Neural Network applications in environmental sciences part I: forward and inverse problems in geophysical remote measurements, Neural Networks, vol 16 (2003), 321-334.

Macke A, Müller J, Raschke E (1996) Single scattering properties of atmospheric ice crystals. Journal of Atmospheric Sciences 53, 2813-2825

Morel, A., and B. Gentili (1991). Diffuse reflectance of oceanic waters: its dependence on sun angle as influence by molecular scattering contribution. Applied Optics, 30, 4427-4438

Mitchell D, Macke A, Liu, Y (1996) Modelling cirrus clouds. part II: Treatment of radiative properties. Journal of Atmospheric Sciences 53, 2967-2988.

Mobley, C.D., Light and Water; Radiative Transfer in Natural Waters (Academic Press, San Diego, Calif., 1994).

Schiller H, Doerffer R (1993) Fast computational scheme for inverse modeling of multispectral radiances: application for remote sensing of the ocean. Applied Optics 32:3280-3285

Schiller, Helmut and Roland Doerffer, 1999, Neural Network for Emulation of an Inverse Model --- Operational Derivation of Case II Water Properties from MERIS data; Int. Journal of Remote Sensing, vol. 20, No 9, 1735—1746.

Shettle, E.P. & R. W. Fenn (1979): Models for the aerosols of the lower atmosphere and the effects of humidity variations on their optical properties. Environmental Research Paper No. 676, AFGL-TR-79-0214, Airforce Geophysics Laboratory

World Climate Research Program (WCRP), (1986): A preliminary cloudless standard atmosphere for radiation computation. International Association for Meteorology and Atmospheric Physics, Radiation Commission, Boulder, CO, USA, 1984, CSP-112, WMO/TD-No. 24, March 1986